Transducer Design for Clamp-on Guided Wave Flow Measurement in Thin-Walled Pipes

Luke Smith, Zhichao Li, and Steve Dixon

***Abstract*—Clamp-on ultrasonic transit time difference flow meters provide opportunities for metering where it is impractical or undesirable to cut into an existing pipeline to install an alternative flow meter. Up until now, it has been difficult to perform this type of measurement on thin-walled metal pipes, due to the difficulty of interpreting the guided wave modes in the combined pipe wall and internal fluid system, but a new method has been reported recently that utilises these guided wave modes for flow measurement. Through computational modelling, and construction and testing of different transducers, the design considerations for clamp-on transducers are highlighted and their impact on guided wave flow rate measurement is evaluated. The design features considered include a curved contact face to provide focusing of the ultrasound within the pipe and a scattering surface to reduce internal reflections. It is found that additional unwanted ultrasonic modes can be minimised by ultrasonic transducer wedge design features such as profiling the curvature of the transducer to conform to the pipe wall or creating a scattering edge to minimise internal wedge reflections. It is also observed that minimising these unwanted modes does not offer any advantage for the transit time difference measurement used in calculating flow.**

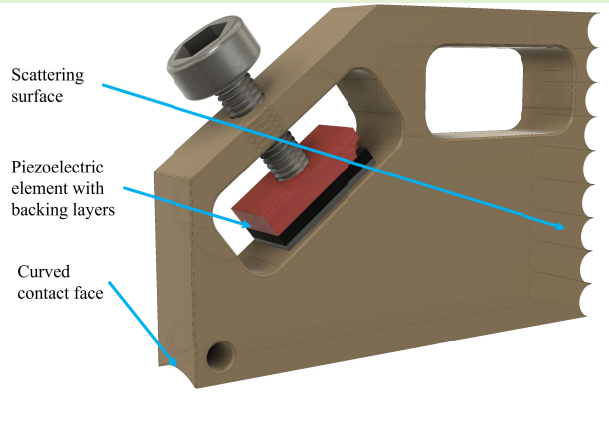

***Index Terms*—Electromechanical sensors, fluid flow measurement, guided wave, Huygens' principle, ultrasonic transducers.**

I. Introduction

THE increasing levels of CO_2 in Earth's atmosphere are giving rise to increased water stress in Europe, which is compounded by an increasing population and changes in water use due to socio-economic development [1]. Over the last century, global fresh water consumption has increased by roughly a factor of 6, and many forecasts agree that consumption is likely to increase in the future [2]. Water metering generally leads to reduced water use compared to unmetered consumers, where in some cases a reduction of 22% is observed [3], [4]. Despite this, installation of water meters has been limited, and even when supplies are metered, readings are not always readily visible to users.

Many types of fluid flow meter are in use throughout the domestic water network and industry, each with their own advantages and disadvantages [5]. Turbine meters are amongst the most common used in metering applications. However, they are not necessarily ideal for national scale retrospective rollout, due to the need to cut into an existing pipe to install the meter, which is disruptive and can incur significant expense. Since turbine meters have moving parts, problems can arise from worn bearings or damaged blades causing poor sensitivity, so it is recommended that they are serviced annually [5].

Clamp-on ultrasonic transit time difference (TTD) flow meters are completely non-invasive and non-intrusive, in that the sensors are not in contact with the fluid, and the pipeline does not need to be cut during installation. Instead, ultrasonic transducers are mounted to the outside of the pipe, and the flow rate is calculated from the time difference between pulses of ultrasound sent upstream and downstream, using suitable assumptions and correction factors [6]. However, current state of the art clamp-on meters have limited capability on small diameter, thin-walled metal pipes, such as those commonly used in domestic and commercial water

Manuscript received March 28, 2022; accepted April 5, 2022. This work was supported in part by the University of Warwick Internal Funds and in part by the Engineering and Physical Sciences Research Council (EPSRC) Impact Acceleration Project under Grant EP/S023275/1. The associate editor coordinating the review of this article and approving it for publication was Prof. Bernhard Jakoby. *(Corresponding author: Luke Smith.)*

Luke Smith and Zhichao Li are with the Department of Physics, University of Warwick, Coventry CV7 7AL, U.K. (e-mail: l.smith.10@warwick.ac.uk; zhichao.li@warwick.ac.uk).

Steve Dixon is with the Department of Physics, School of Engineering, University of Warwick, Coventry CV4 7AL, U.K. (e-mail: s.m.dixon@warwick.ac.uk).

The data presented in this article can be accessed via the IEEE DataPort DOI: 10.21227/ag6z-ck74

Digital Object Identifier 10.1109/JSEN.2022.3169283

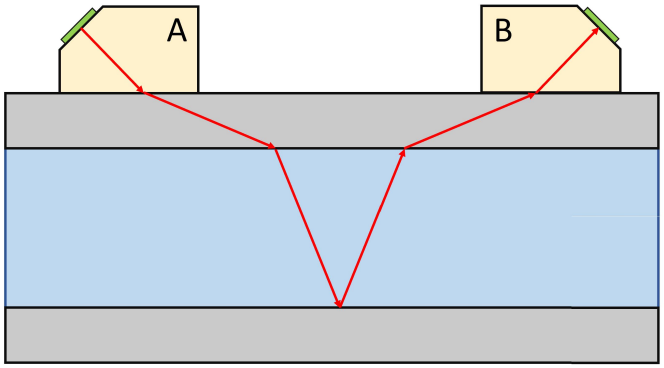

Fig. 1. Schematic diagram of a clamp-on ultrasonic flow meter. Transducers A and B are fixed to the outside of the pipe (grey) and the ultrasonic path is shown in red. Note that additional ultrasonic echoes may arise in the upper and lower pipe walls but are not shown here, as they can usually be neglected.

supplies. The generation of guided waves in the combined pipe wall-liquid system complicates the received signal, typically resulting in an inability to reliably measure flows less than 32 ml·s^{-1}, commonly with an accuracy less than ±50% [7].

In previous work, a technique for performing clamp-on TTD measurements with miniature sensors has been demonstrated. Using this technique, flow rate measurements down to 1.25 ml· s^{-1} have been achieved with an error of only 1% [7]. In the work documented in this paper, the effect of features including scattering surfaces and curved contact faces are evaluated via Huygens modelling and experiment.

II. Theory

TTD ultrasonic flow meters calculate the flow rate in a pipe by measuring the transit time difference between pulses of ultrasound sent upstream and downstream. The transducers can be in direct contact with the fluid, also known as 'wetted', or they can be situated on the exterior of an existing pipe, called 'clamp-on'.

Fig. 1 shows a schematic diagram of a clamp-on flow meter. The piezoelectric element in transducer A, shown in green, will be driven to emit a pulse of ultrasound which mode converts to a shear wave in the pipe wall, with the angle of refraction determined by Snell's law. The angle of the transducer wedge is usually chosen such that the angle of incidence is beyond the critical angle for the compression wave [8]. At the pipe wall - fluid boundary, the shear wave is mode converted again into a compression wave in the fluid. After reflecting off the bottom of the pipe, the ultrasound follows the inverse path back to transducer B, where it is detected as a voltage across the piezoelectric element. This process is then repeated but with the generation and receiving transducers switched, and the time difference between the upstream and downstream arrivals is measured. The time difference between the arrivals arises because ultrasound travelling upstream has a component of its velocity opposed to the flow direction, and the pulse travelling downstream has a component travelling with the flow. It is therefore expected that the downstream transit time will be shorter than the upstream transit time [9].

Fig. 2 shows a simulated pair of pulses from the system in Fig. 1, where the TTD is 20ns. It can be shown that the

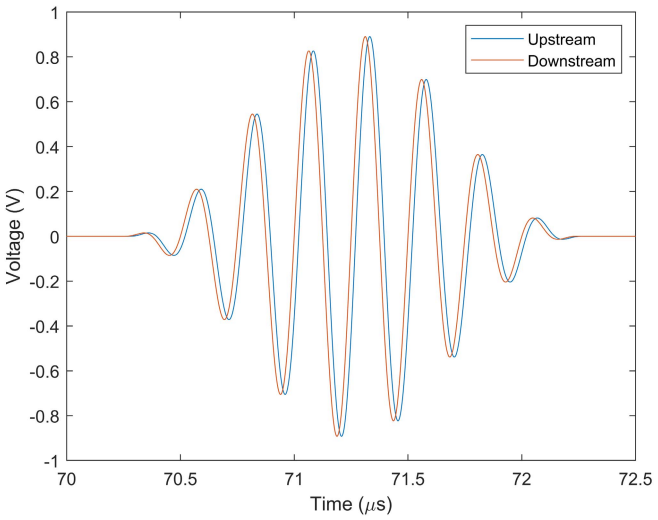

Fig. 2. A simulated pair of received signals from a clamp-on transducer on a thick-walled pipe with a time difference of 20 ns.

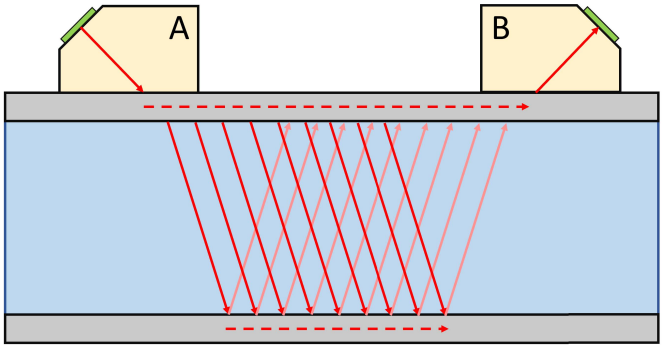

Fig. 3. Schematic diagram showing the propagation of a guided wave mode through a thin-walled pipe in a clamp-on ultrasonic flow meter. The guided waves are represented by the dashed lines which continuously leak energy out into the fluid.

relationship between the flow velocity, v_l, and the TTD, Δt, is given by [8], [9]

$$v_l = \frac{k c_l^2 \Delta t}{2D \tan(\theta_i)} \tag{1}$$

where c_l is the speed of sound in the liquid, D is the interior diameter of the pipe, and θ_i is the angle of incidence into the water. There is also a correction factor, k. This appears because the flow profile is not constant over the area of the pipe, and the flow meter measures an average over the line of the ultrasonic path, rather than the area average that is required for calculating the volumetric flow rate [10].

In the thin-walled pipes considered in this research, the received signal is complicated by the presence of guided waves in the pipe wall – liquid system [7]. Fig. 3 shows a 2D schematic representation of one guided wave mode propagating through the system. In this mode, ultrasonic energy propagating along the top wall of the pipe is continuously leaking out into the fluid, and similarly ultrasonic wavefronts in the water transfer energy to the pipe wall. A similar process occurs on the opposite pipe wall, except initially the ultrasonic wavefront in the fluid feeds energy into the pipe wall. This process arises along the length of the fluid filled pipe between

the transducers, and an ultrasonic wave is eventually detected by the receiving transducer. The corresponding pulse that is seen at the receiving transducer can be viewed as arising from all of the possible paths through the system that take the same amount of time [7]. This mode will henceforth be referred to as the "1V" mode, since the ultrasound travels once downwards and once upwards through the fluid. Higher order modes will also be present in the received signal. For example, the "2V" mode results from ultrasound that has been through the fluid four times in two "V-shaped" paths, and so on.

The transducers typically used in clamp-on flow meters usually have a flat face which forms a line contact with the pipe, so one would expect that diffraction in the pipe cross-section causes some energy to take a chordal path through the fluid. The same is true for larger diameter, thick-walled pipes, but in that case waves that do not travel along the pipe diameter do not make a significant contribution to the signal detected by the receiving transducer, so this effect is often safely neglected. In the small diameter, thin-walled metal pipes, it is expected that ultrasonic energy that has taken a chordal path across the pipe will contribute to the received ultrasonic signal [7].

One could speculate that the modes that are most strongly detected would correspond to a ray tracing path that might have a perspective view looking down the length of the pipe as a triangular or even square arrangement, but we would expect the amplitude of such modes to be significantly lower than the "V" modes. This is what is experimentally observed, but creating a finite element model to simulate this has not yet been possible due to the large number of nodes required [7]. These chordal path modes are labelled as "1T", "2T" and so on, where the order describes how many triangles are included in the ultrasonic path. Similarly, one could imagine a square shaped set of paths denoted "1S", "2S" and even possibly and a pentagonal set, denoted "1P", "2P" or higher order polynomial shapes.

Equation (1) for the calculation of the flow rate is only applicable to the 1V mode. It is relatively simple to derive equations for different shaped or higher order modes, but in order to make a flow measurement using them, the arrivals must be matched with the path they have taken through the system. Additionally, it is imperative to ensure that any ultrasonic arrival that is being used for flow measurement consists of only one mode.

III. Computer Modelling

Two computer models have been developed to gain an understanding of how ultrasound travels through the system, and the insight gained aids the design of the new transducers.

A. Ray Tracing Model

For a path in the plane of the transducers such as that shown in Fig. 3, calculating the arrival time of different modes by hand is simple. However, when considering lots of out of plane paths it becomes unfeasible, so a computer model was developed to automate the process.

The first of the two models uses a ray tracing approach to calculate predicted arrival times for different paths in three dimensions under zero flow conditions. For each mode, the time for only one path is simulated because in a single mode, all of the possible paths should have the same transit time. The model sets up an initial ray originating normally from the piezoelectric element, then at each material boundary, calculates the refracted or reflected waves, or initiates a guided wave. In previous work, it has been shown that despite the wall thickness being thin compared to the wavelength, Snell's law still applies for the angle of refraction into the fluid from the transducer [7]. This process repeats until either the mode misses the receiving transducer, in which case the path is discarded, or it is detected. Once the distance travelled in each material is known, it is trivial to calculate the transit time of that particular mode.

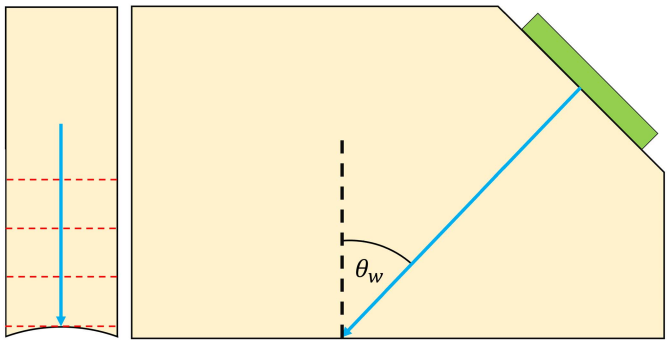

Fig. 4. A schematic diagram of a wedge transducer showing plane waves from the piezoelectric element (green) impinging on a curved contact face.

B. Huygens Modelling

The use of Huygens principle in transducer design is widespread, as it predicts beam shapes with relatively little computational expense. In this research, a Huygens model was constructed to model the beam spread in the cross-section of the pipe by setting sources along the contact face of the transducer wedge. By summing the waves emitted from the interface, the beam shape within the pipe can be calculated [11]. Since the piezoelectric element will excite plane waves in the transducer wedge, if the contact face is curved, the phase of the sources must be considered. A schematic diagram of a transducer with a curved contact face is shown in Fig. 4. The phase difference ϕ between two sources is given by [12]

$$\phi = \frac{2\pi\,\Delta r}{\lambda}, \tag{2}$$

where λ is the wavelength of the ultrasound and Δr is the difference between the distance to each of the sources. Dividing the numerator and denominator by the sound speed gives

$$\phi = \frac{2\pi\,\Delta r}{cT} = 2\pi f(t - t_0), \tag{3}$$

where f is the ultrasonic frequency, c is the sound speed, T is the period of the wave, t is the time the wavefront hits a given point on the interface and t_0 is a reference time for which the phase is set to zero. For a source at height y on the arc of radius R pictured in Fig. 4, the phase difference is given by

$$\phi = \frac{2\pi f(R - y)}{c_y} = \frac{2\pi f(R - y)}{c_w \cos(\theta_w)}, \tag{4}$$

where $c_y = c_w \cos(\theta_w)$ is the component of the wave speed in the vertical direction in the wedge, c_w is the sound speed in the wedge, and θ_w is the wedge angle as shown in fig. 4. The phase difference has been set to zero at the top of the arc (in the centre of the wedge), where $R = y$.

The sources were set out along the contact face of the transducer with a density of 100 sources/mm and the radiation pattern was calculated in a plane cutting through the pipe at the refraction angle into the water. Interactions with the pipe walls are not considered.

IV. Methodology

The computational models were verified with experiments on a 15 mm outer diameter, 0.7 mm wall thickness copper pipe for each design of transducer. The polyether ether ketone (PEEK) transducers are fixed to the pipe in a 3D printed mount with the centre points of the piezoelectric elements separated by 79 mm. A small amount of gel couplant is applied to the contact faces of the transducers before mounting. The generation transducer was driven with a 10 V pk-pk, 5-cycle, 4 MHz sinewave burst from a Tektronix AFG3102C arbitrary function generator and the received signal was detected with a Tektronix DPO2014 oscilloscope after preamplification by 20 dB with an Olympus 5077PR.

Measurements at non-zero flow were then conducted to determine the effect of the different designs on the precision of flow rate measurements. Flow rate measurements were conducted on a flow rig capable of flow rates up to $\sim$100 ml·s^{-1}, and the true flow rate was determined by weighing volumes of water collected over a specified time. Transit time differences were calculated from the upstream and downstream signals using a cross-correlation technique with interpolation to increase sensitivity and Savitzky-Golay filtering to remove digitisation noise [13]. At each flow rate, six transit time differences were calculated from the six V mode arrivals.

After converting these to the equivalent 1V mode times and removing the zero-flow offset, a weighted mean was taken with weights determined by the inverse of the standard deviation around a straight line fit for each arrival. This best estimate of the TTD was then used to calculate a flow rate using (1) with a correction factor $k = 1$.

V. Results and Discussion

Six different transducer designs were created with the aim to simplify the received signal so that only arrivals which could be used for flow measurement were visible. Specifically, avoiding arrivals that contain more than one mode is important as they will have different TTDs. Also considered were the ease of manufacturing and material costs.

Fig. 5 shows the six designs that were tested. The design shown in Fig. 5(a) is the original design that was reported in reference [14], but without the scattering surface. Design (a) represents the simplest solution for comparison with the other designs. This is already a very small sensor compared to those conventionally used for clamp on flow measurement at only 6.5 mm wide. The small holes at the base of the transducer wedge are for mounting in a rail on the pipe. However, it was found that with a more rigid design of transducer mount, the friction between the sides of the transducer and the mount was sufficient to maintain an adequate amount of pressure on the pipe. To reduce the probability of internal reflections, the mounting holes were removed and a scattering face was added

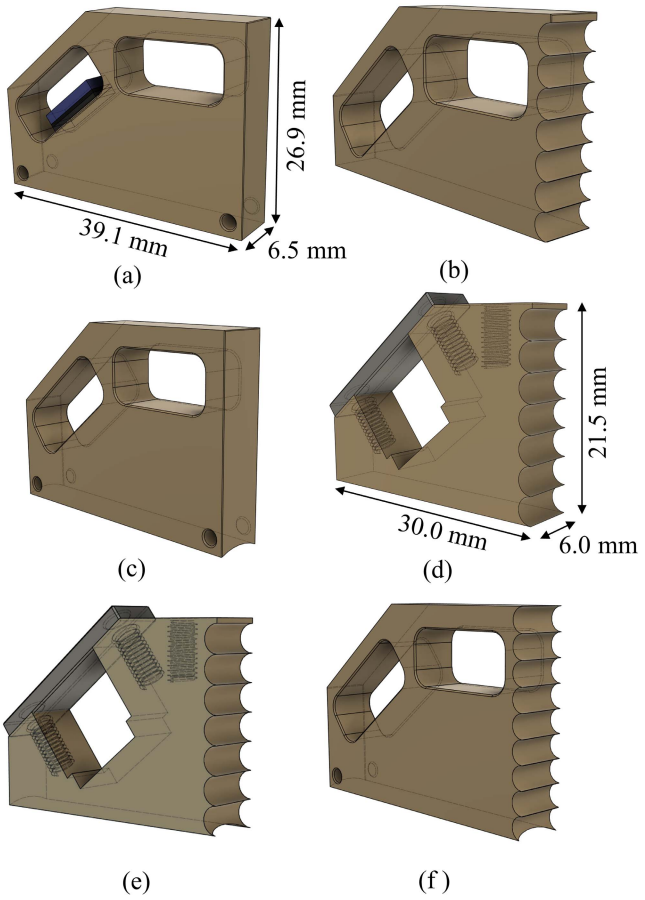

Fig. 5. Computer aided design (CAD) models of the six different transducer designs. (a) A simple miniature transducer similar to that presented in [14] but with no scattering surfaces, with the piezoelectric and backing material shown. (b) A modified version of (a) with the holes removed from the bottom and a scattering face added. (c) A modified version of (a) with a curved contact face to match the curvature of the pipe. (d) A new, even smaller design with a scattering face. (e) A modified version of (d) with a curved contact face. (f) A modified version of (a) with a curved contact face and a scattering face.

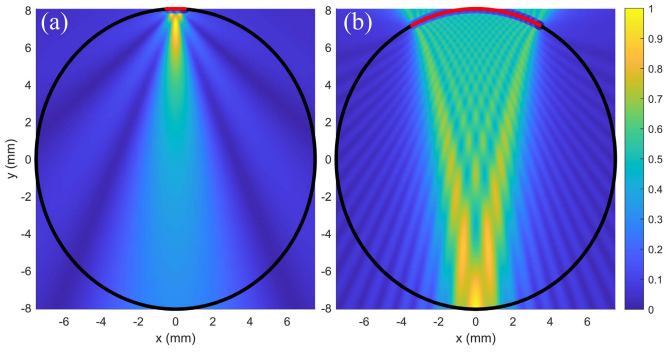

Fig. 6. Huygens simulation results in a plane inclined at 22° to the vertical intercepting the pipe (black) to match the angle of refraction into the fluid. The sources (red) are 1 mm wide and flat in (a) to emulate a narrow contact, as with the flat faced transducer wedges. In (b), the sources are curved across the top of the pipe and are 6.5 mm wide to emulate the full width of the transducer being in ultrasonic contact with the pipe. The colour bar units are normalised amplitude units.

in design (b). Since the face of the transducer that contacts the pipe is flat and the pipe surface is curved, only a narrow region is in ultrasonic contact. This will produce a relatively wide beam in the cross-section of the pipe compared to a wider contact, so a curved face to match the curvature of the pipe was added in design (c). Design (f) is a combination of (b) and (c), with both the curved contact face and the scattering face. Designs (d) and (e) are smaller than the other designs, so they require ∼45% the amount of PEEK material. They are also simpler to machine as they have no enclosed holes, although in mass production all of the designs are small enough to be injection moulded [14]. Both (d) and (e) have the scattering face to reduce internal reflections; the contact face of (d) is flat, whilst that of (e) also features the curved contact face.

To predict whether the curved contact face in designs (c), (e) and (f) would have the desired focusing effect, Huygens simulations were conducted as described in section III for the sound field entering the pipe. The results are shown in Fig. 6 for both the narrow line contact and the full width contact for the curved faced transducer designs. Note that this is calculated for an infinite plane, so energy being reflected from the inner pipe walls is not considered. Therefore, Fig. 6 only shows the ultrasound field on the first transit through the fluid. The black ellipse superimposed on Fig. 6(a) and 6(b) is to indicate where the pipe cross section would be.

Fig. 6(a) clearly shows the ultrasonic energy spreading out within the cross-section, which could give rise to modes such as the T, S and P modes discussed previously. Fig. 6(b) shows that the intensity of ultrasound incident on the pipe directly under the transducer is increased when the curved contact face is used, which might be expected to increase the signal to noise ratio in the V mode arrivals and decrease the amplitude of the T, S and P modes.

Fig. 7 shows the logarithm of the envelope of the received signals using each of the different transducers shown in Fig. 5, along with the predicted arrival times from the ray tracing model. The signals initially had their main arrivals misaligned due to small differences in the amount of PEEK material between the piezoelectric and pipe surface, so they were aligned in post-processing for easier comparison. The signals were normalised such that their largest arrival had an amplitude of one unit, then a DC offset of 0.1 units was added before taking the logarithm so that the result is constrained to the range -1 to 0.

In all six panels, the six most prominent ultrasonic arrivals align well with the predicted times for the V modes. For the later V modes the arrivals are slightly misaligned with the predictions because the predicted arrival time has a greater dependence on the speed of sound in the water, which is dependant on the temperature. For the other modes, the predicted arrival times are often close to each other, making it difficult to assign particular modes to the smaller arrivals. Additionally, the ray tracing model does not account for beam spread, so some higher order modes may have been calculated to miss the receiving transducer when they were detected in the experiment. However, generally the introduction of scattering surfaces and curved contact faces does appear to reduce the amplitude of the smaller arrivals in Fig. 7. If there were other modes present in the V mode arrivals for design (a), this may indicate that the amplitudes of these other modes would be reduced in designs (e) and (f), which could be beneficial for flow measurement.

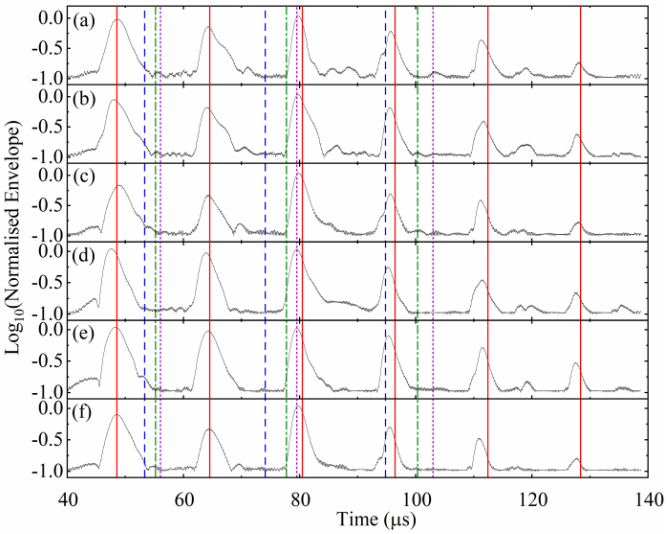

Fig. 7. The envelope of the received signals using the six different transducer designs from Fig. 5 plotted on a logarithmic scale. The piezoelectric - piezoelectric separation was 79 mm. Panel (a) shows the received signal using transducer design (a), panel (b) shows the received signal using transducer design (b), panel (c) corresponds to design (c), panel (d) corresponds to design (d), panel (e) corresponds to design (e), and panel (f) corresponds to transducer design (f). The vertical lines are the predicted arrival times from the ray tracing model. Red, solid: V modes. Blue, dashed: T modes. Green, dot-dashed: S modes. Purple, dotted: P modes. Higher order modes appear later in time.

To test whether the new designs translated into an improved transit time difference flow measurement, a series of flow measurements were then taken using the six different transducer designs. Since zero flow offset and gradients that deviate from unity can be compensated for during processing, the amount of scatter around a straight line fit was taken to be a good measure of transducer performance. It can be seen from the residual plot panels in Fig. 8, that the scatter around a straight line generally decreases slightly with increasing flow rate. This is expected as the time difference measurement increases with increased flow while the trigger time jitter and the digitisation rate is the same for all flow rates. This poses a problem when using statistical measures of scatter such as the standard deviation, as the result will be skewed towards higher values if more measurements are taken at low flow rates, and vice versa if more measurements are taken at high flow rates. One way to reduce this effect is to use a standard deviation weighted by the flow rates. This puts a higher weight on high flow rates, where the scatter around a straight line fit appears to be more consistent, but also provides less indication of the performance at low flow rates. The resulting figure of merit is shown with the dashed lines in the residual sub-panels. The weighted standard deviations for the six transducer designs are listed in Table I.

From the weighted standard deviations in Table I and the residual plots in Fig. 8, it is clear that the original design showed the best performance in these tests, contrary to

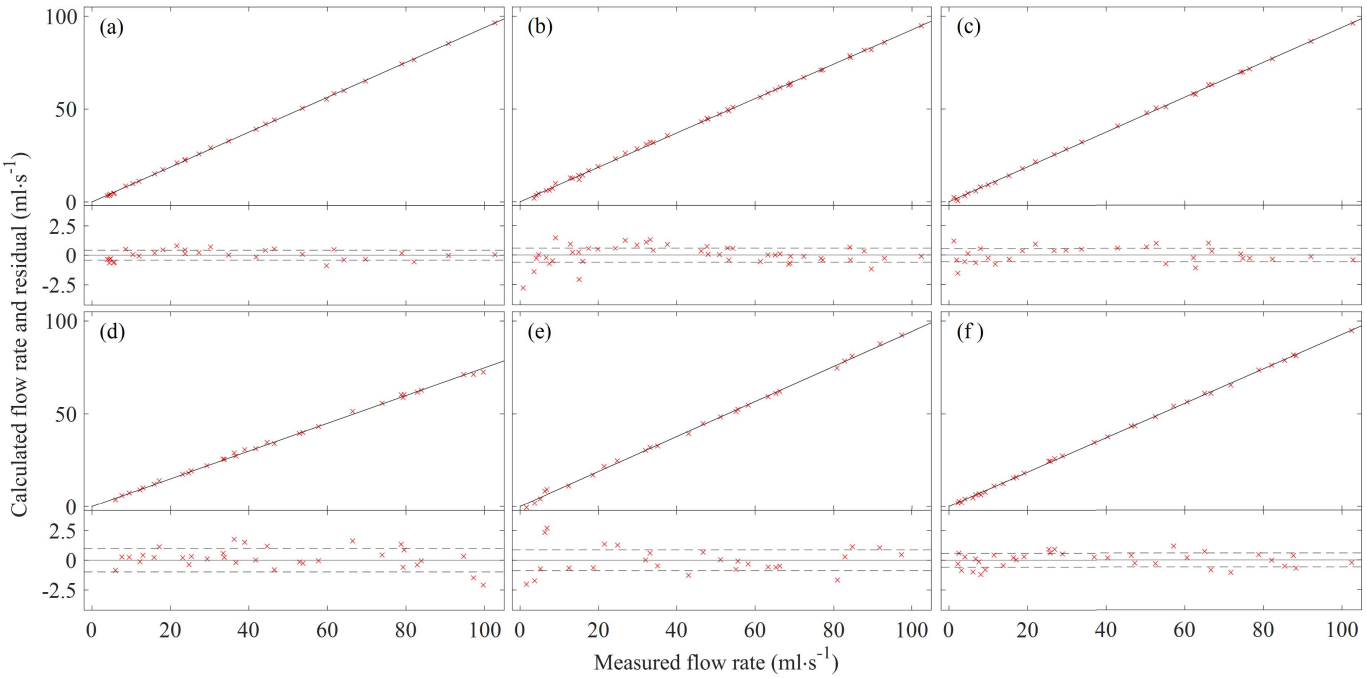

Fig. 8. Flow rate measurements using six different clamp-on transducer designs. Panel (a) shows data taken with transducer design (a) from Fig. 5, panel (b) shows data taken using transducer design (b), panel (c) was with design (c), panel (d) was with design (d), panel (e) was with design (e) and panel (f) was with design (f). Each large panel is split into two sub-panels: the top is the measured flow rate, and the bottom is the residuals after fitting with a straight line. The dashed lines in the bottom sub-panels indicate the standard deviation of the residuals weighted by flow rate.

TABLE I
TRANSDUCER PERFORMANCE METRIC

Transducer Design	Weighted Standard Deviation ($ml \cdot s^{-1}$)
(a)	0.418
(b)	0.611
(c)	0.568
(d)	0.990
(e)	0.875
(f)	0.589

Weighted standard deviation of calculated flow rates around a straight line fit from six different transducer designs shown in Fig. 5. Weights are equal to the measured flow rates.

expectations based on the appearance and apparently improved mode purity seen in Fig. 7 for waveforms (c), (d), (e) and (f) when compared to waveform (a). The reasons for this apparent contradiction could be due to the limitations of the models. For example, the Huygens model only shows the behaviour of ultrasound when it first enters the pipe, and it ignores any guided wave effects from ultrasonic energy spreading out circumferentially around the pipe wall. This is clearly a large effect to ignore in this case, where the guided waves form the basis of the technique. While some focussing may be achieved before the first reflection, the effect of the transducer's curved face on the subsequent transits through the fluid are unobtainable using this technique. To take all of these effects into account, a three-dimensional finite element model is required. Another possibility is that the scatter about a straight line is actually dominated by another factor such as the coupling to the pipe, temperature differences in the fluid, electrical noise, or the clamping force on the piezoelectric element. Since the weighted standard deviations are quite close in value for most of the designs, it is feasible that these other factors play a role in deciding which transducers appear to be optimal.

VI. CONCLUSION

Six different transducer designs have been constructed and tested for clamp-on guided wave transit time difference flow measurement in 15 mm diameter copper pipes with a wall thickness of 0.7 mm. Through the use of computational modelling, the highest amplitude ultrasonic arrivals were characterised in terms of the paths the ultrasound had taken to reach the detection transducer. It has been demonstrated that the curved contact face and the addition of a scattering surface appear to reduce the number of unwanted guided wave modes in the received signal in the thin-walled clamp-on system, but this does not necessarily lead to increased flow measurement performance. Instead, a variety of other factors related to the transducer construction, coupling to the pipe and temperature variations could dominate the precision with which flow measurements can be made. It should also be noted that the difference in the weighted standard deviations are extremely small, all being less than 1 ml s^{-1}. Therefore, the benefits of using a transducer with a flat contact face, such as ease of manufacture and the ability to operate on any pipe size, outweigh any possible benefits of the curved contact face for the pipes tested.

Many further research opportunities have been identified. Firstly, the method of clamping the transducers to the exterior of the pipe is expected to have a large influence on both the quality of the ultrasonic contact with the pipe, and the period of time over which a sufficient level of contact can be maintained. Secondly, the backing materials and clamping mechanism used to secure the piezoelectric elements in

the transducers will impact the received pulse duration and amplitude, and the frequency response of the transducer. Methods with adjustable clamping force provide opportunities for matching the transducer responses, but they also allow for changes in the clamping conditions over time. A better understanding of these considerations will allow them to be controlled so that the effects of the different designs on flow measurements can be determined. More comprehensive modelling will also result in a better picture of the differences in performance, since it will provide a more complete view of how the focussing wedges affect the ultrasonic transit through the system.

ACKNOWLEDGMENT

The authors would like to acknowledge Jonathan Harrington, with the Mechanical Workshop at the University of Warwick, for creating the PEEK transducer wedges.

REFERENCES

[1] T. Henrichs, B. Lehner, and J. Alcamo, "An integrated analysis of changes in water stress in Europe," *Integr. Assessment*, vol. 3, no. 1, pp. 15–29, Mar. 2002, doi: 10.1076/iaij.3.1.15.7406.

[2] United Nations. (Mar. 21, 2021). *UN World Water Development Report 2021: Valuing Water*. UN Educational, Scientific and Cultural Organization. Paris, France. Accessed: Jan. 10, 2022. [Online]. Available: https://unesdoc.unesco.org/ark:/48223/pf0000375724

[3] M. van Vugt and C. D. Samuelson, "The impact of personal metering in the management of a natural resource crisis: A social dilemma analysis," *Personality Social Psychol. Bull.*, vol. 25, no. 6, pp. 735–750, Jun. 1999, doi: 10.1177/0146167299025006008.

[4] C. Ornaghi and M. Tonin, "The effects of the universal metering programme on water consumption, welfare and equity," *Oxford Econ. Papers*, vol. 73, no. 1, pp. 399–422, Nov. 2019, doi: 10.1093/oep/gpz068.

[5] R. Baker, *Flow Measurement Handbook*, 2nd ed. Cambridge, U.K.: Cambridge Univ. Press, 2016.

[6] M. L. Sanderson and H. Yeung, "Guidelines for the use of ultrasonic non-invasive metering techniques," *Flow Meas. Instrum.*, vol. 13, no. 4, pp. 125–142, Aug. 2002, doi: 10.1016/s0955-5986(02)00043-2.

[7] S. Dixon, Z. Li, M. Baker, X. Bushi, and L. Smith, "Clamp-on measurements of fluid flow in small-diameter metal pipes using ultrasonic guided waves," *IEEE Trans. Instrum. Meas.*, vol. 70, pp. 1–3, Oct. 2021, doi: 10.1109/TIM.2021.3120142.

[8] Z. Li, F. Hughes, N. C. Kerr, R. Wilson, and S. Dixon, "Liquid flow measurement using silicone polymer wedge clamp-on ultrasonic transducers," *IEEE Trans. Instrum. Meas.*, vol. 69, no. 7, pp. 5157–5165, Jul. 2020, doi: 10.1109/tim.2019.2954235.

[9] A. Hamouda, O. Manck, M. L. Hafiane, and N.-E. Bouguechal, "An enhanced technique for ultrasonic flow metering featuring very low jitter and offset," *Sensors*, vol. 16, no. 7, p. 1008, Jun. 2016, doi: 10.3390/s16071008.

[10] B. Iooss, C. Lhuillier, and H. Jeanneau, "Numerical simulation of transit-time ultrasonic flowmeters: Uncertainties due to flow profile and fluid turbulence," *Ultrasonics*, vol. 40, no. 9, pp. 1009–1015, 2002, doi: 10.1016/s0041-624x(02)00387-6.

[11] J. Rose, "Guided waves in viscoelastic media," in *Ultrasonic Waves Solid Media*, 1st ed. Cambridge, U.K.: Univ. Press, 1999, p. 338.

[12] H. Young, R. Freedman, L. Ford, F. Sears, and H. Young, "Interference," in *University Physics With Modern Physics*, 15th ed. Harlow, U.K.: Pearson, 2019, p. 1168.

[13] W. H. Press and S. A. Teukolsky, "Savitzky-Golay smoothing filters," *Comput. Phys.*, vol. 4, no. 6, p. 669, Nov./Dec. 1990, doi: 10.1063/1.4822961.

[14] Z. Li, L. Smith, and S. Dixon, "Design of miniature clamp-on ultrasonic flow measurement transducers," *IEEE Sensors Lett.*, vol. 5, no. 6, pp. 1–4, Jun. 2021, doi: 10.1109/LSENS.2021.3081760.